Alpha Decay Width of ^{212}Po from a quartetting wave function approach

Chang Xu,[1,*] Zhongzhou Ren,[1,2,†] G. Röpke,[3,‡] P. Schuck,[4,5,§] Y. Funaki,[6] H. Horiuchi,[7,8] A. Tohsaki,[7] T. Yamada,[9] and Bo Zhou[7]

[1] *Department of Physics and Institute of Acoustics, Nanjing University, Nanjing 210093, China*
[2] *Center of Theoretical Nuclear Physics, National Laboratory of Heavy-Ion Accelerator, Lanzhou 730000, China*
[3] *Institut für Physik, Universität Rostock, D-18051 Rostock, Germany*
[4] *Institut de Physique Nucléaire, Université Paris-Sud, IN2P3-CNRS, UMR 8608, F-91406, Orsay, France*
[5] *Laboratoire de Physique et Modélisation des Milieux Condensés, CNRS- UMR 5493, F-38042 Grenoble Cedex 9, France*
[6] *RIKEN Nishina Center, Wako 351-0198, Japan*
[7] *Research Center for Nuclear Physics (RCNP), Osaka University, Osaka 567-0047, Japan*
[8] *International Institute for Advanced Studies, Kizugawa 619-0225, Japan*
[9] *Laboratory of Physics, Kanto Gakuin University, Yokohama 236-8501, Japan*

(Dated: August 14, 2016)

A microscopic calculation of α-cluster preformation probability and α decay width in the typical α emitter ^{212}Po is presented. Results are obtained by improving a recent approach to describe α preformation in ^{212}Po [Phys. Rev. C **90**, 034304 (2014)] implementing four-nucleon correlations (quartetting). Using the actually measured density distribution of the ^{208} Pb core, the calculated alpha decay width of ^{212}Po agrees fairly well with the measured one.

PACS numbers: 21.60.-n, 21.60.Gx, 23.60.+e, 27.30.+w

arXiv:1511.07584v1 [nucl-th] 24 Nov 2015

* cxu@nju.edu.cn
† zren@nju.edu.cn
‡ gerd.roepke@uni-rostock.de
§ schuck@ipno.in2p3.fr

The radioactive α decay is a frequent phenomenon in nuclear physics, in particular near the doubly magic nuclei ^{100}Sn and ^{208}Pb, and the superheavies where α decay competes with spontaneous fission (for a recent discussion see [1] and refs. given there). Whereas the tunneling of an α particle across the Coulomb barrier is well described in quantum physics, the problem in understanding the α decay within a microscopic approach is the preformation of the α cluster in the decaying nucleus.

The formation of α-like correlations in nuclear systems has been investigated recently. In particular, in light, low density states of selfconjugate nuclei (^{8}Be, ^{12}C, ^{16}O, ^{20}Ne, etc.) four-nucleon correlations have been identified within the THSR (Tohsaki-Horiuchi-Schuck-Röpke) approach [2], but also with other theories like Resonating Group Method (RGM) [3], Brink-GCM (Generator Coordinate Method) [4], Fermion Molecular Dynamics (FMD) [5], Antisymmetrised Molecular Dynamics (AMD) approaches [6] going beyond the mean-field approximation. The main message is that well-defined clusters are formed only in regions where the density of nuclear matter is low. Therefore, it is of interest to investigate α-like correlations also in the outer tails of the density of a nucleus, and α preformation is discussed as a surface effect confined to the region where the nucleon density is comparable or below 1/5 of saturation density $n_{\rm sat} = 0.16$ fm^{-3}.

A typical example is ^{212}Po which is an α emitter with half-life 0.299 μs and decay energy $Q_\alpha = 8954.13$ keV. It is spherical, doubly magic, and has only one decay channel. Several approaches have been made to calculate the α decay width of ^{212}Po within a microscopic approach, see Ref. [7] and refs. therein. Furthermore a quartetting wave function approach has been worked out recently [8]. Performing various approximations, exploratory calculations resulted in a preformation factor of about 0.37.

Here, we are interested in the α decay width of ^{212}Po. The transition probability for the α decay $W = P_\alpha \nu \mathcal{T}$ is given as product of the preformation probability P_α, the frequency (pre-exponential factor) ν, and the exponential factor $\mathcal{T}$. In the present work, we improve the exploratory calculation performed in [8] replacing simple expressions for the density and the potentials by more realistic ones. We refine the calculation of the quartetting state using recently measured density profiles for the ^{208}Pb core [9]. Furthermore, we improve the mean-field potential using the M3Y double-folding potential, see [10], instead of the Woods-Saxon potential. To evaluate the α decay width, we use the approach of Gurvitz [11] to estimate the preexponential factor. In addition to the preformation factor and the binding energy, results for the half-life will be given.

Preformation probability. An effective α particle equation has been derived recently [8] for cases where an α particle is bound to a doubly magic nucleus. As an example, ^{212}Po has been considered which decays into a ^{208}Pb core and an α particle. Neglecting recoil effects, we assume that the core nucleus is fixed at $\mathbf{r} = 0$. The core nucleons are distributed with the baryon density $n_B(r)$ and produce a mean field $V_\tau^{\rm mf}(r)$ acting on the two neutrons ($\tau = n$) and two protons ($\tau = p$) moving on top of the lead core. In the present work, we will not give a microscopic description of the core nucleons (e.g., Thomas-Fermi or shell model calculations) but consider both $n_B(r)$ and $V_\tau^{\rm mf}(r)$ as phenomenological input. Of interest is the wave function of the four nucleons on top of the core nucleus which can form an α-like cluster.

The four-nucleon wave function (quartetting state) $\Psi(\mathbf{R}, \mathbf{s}_j) = \varphi^{\rm intr}(\mathbf{s}_j, \mathbf{R})\, \Phi(\mathbf{R})$ is subdivided in a unique way in the (normalized) center of mass (c.m.) part $\Phi(\mathbf{R})$ depending only on the c.m. coordinate $\mathbf{R}$, and the intrinsic part $\varphi^{\rm intr}(\mathbf{s}_j, \mathbf{R})$ which depends, in addition, on the relative coordinates $\mathbf{s}_j$ (for instance, Jacobi-Moshinsky coordinates) [8]. The respective c.m. and intrinsic Schrödinger equations are coupled by contributions containing the expression $\nabla_R \varphi^{\rm intr}(\mathbf{s}_j, \mathbf{R})$ which will be neglected in the present work. In contrast to homogeneous matter where this expression disappears, in finite nuclear systems such as ^{212}Po this gradient term will give a contribution to the wave equations for $\Phi(\mathbf{R})$ as well as for $\varphi^{\rm intr}(\mathbf{s}_j, \mathbf{R})$. Up to now, there are no investigations of such gradient terms.

The intrinsic wave equation describes in the zero density limit the formation of an α particle with binding energy $B_\alpha = 28.3$ MeV. For homogeneous matter, the binding energy will be reduced because of Pauli blocking. In the zero temperature case considered here, the shift of the binding energy is determined by the baryon density $n_B = n_n + n_p$, i.e. the sum of the neutron density n_n and the proton density n_p. Furthermore, Pauli blocking depends on the asymmetry given by the proton fraction n_p/n_B and the c.m. momentum $\mathbf{P}$ of the α particle. Neglecting the weak dependence on the asymmetry, for $\mathbf{P} = 0$ the density dependence of the Pauli blocking term $W^{\rm Pauli}(n_B) = 4515.9\, n_B - 100935\, n_B^2 + 1202538\, n_B^3$ was found in [8], Eq. (45), as a power expansion with respect to n_B. In particular, the bound state is dissolved and merges with the continuum of scattering states at the Mott density $n_B^{\rm Mott} = 0.02917$ fm^{-3}.

The intrinsic wave function remains nearly α-particle like up to the Mott density (a small change of the width parameter b of the four-nucleon bound state is shown in Fig. 2 of Ref. [8]), but becomes a product of free nucleon wave functions (more precisely the product of scattering states) above the Mott density. This behavior of the intrinsic wave function will be used below when the preformation probability for the α particle is calculated. Below the Mott density the intrinsic part of the quartetting wave function has a large overlap with the intrinsic wave function of the free α particle. In the region where the α-like cluster penetrates the core nucleus, the intrinsic bound state wave function transforms at the critical density $n_B^{\rm Mott}$ into an unbound four-nucleon shell model state.

In the case of ^{212}Po considered here, an α particle is moving on top of the doubly magic ^{208}Pb core. The tails of the density distribution of the Pb core where the baryon density is below the Mott density $n_B^{\rm Mott}$, is relevant for the

formation of α-like four-nucleon correlations. Simply spoken, the α particle can exist only at the surface of the heavy nucleus. This peculiarity has been considered since a long time for the qualitative discussion of the preformation of α particles in heavy nuclei [1, 12, 13]. It has recently also been discussed in connection with the neutron skin thickness of heavy nuclei with α-particle correlations [14].

Improving simple estimations (Thomas-Fermi model as well as the Shlomo parametrization of the density) for the baryon density considered in [8], we use the empirical results obtained recently [9] which are parametrized by Fermi functions. With the neutron density $n_n(r) = 0.093776/\{1 + \exp[(r - 6.7\text{fm})/0.55\text{fm}]\}\text{fm}^{-3}$ and the proton density $n_p(r) = 0.062895/\{1 + \exp[(r - 6.68\text{fm})/0.447\text{fm}]\}\text{fm}^{-3}$, the Mott density $n_B^{\rm Mott} = 0.02917$ fm^{-3} occurs at $r_{\rm cluster} = 7.4383$ fm, $n_B(r_{\rm cluster}) = n_B^{\rm Mott}$. This means that α-like clusters can exist only at distances $r > r_{\rm cluster}$, for smaller values of r the intrinsic wave function is characterized by the uncorrelated motion.Note that this transfer of results obtained for homogeneous matter to finite nuclei is based on a local density approach. In contrast to the weakly bound di-nucleon cluster, the α particles are more compact so that a local-density approach seems to be better founded. However, the Pauli blocking term is non-local. As shown in [8], the local density approach can be improved systematically. It is expected that non-local interaction terms and gradient terms will make the sudden transition at $r_{\rm cluster}$ from the intrinsic α-like cluster wave function to an uncorrelated four-nucleon wave function more smooth.

Our main attention is focussed on the c.m. motion $\Phi(\mathbf{R})$ of the four-nucleon wave function (quartetting state of four nucleons $n_\uparrow, n_\downarrow, p_\uparrow, p_\downarrow$). Because the lead core nucleus is very heavy, we replace the c.m. coordinate $\mathbf{R}$ by the distance r from the center of the ^{208}Pb core. The corresponding Schrödinger equation contains the kinetic part $-\hbar^2\nabla_r^2/8m$ as well as the potential part $W(\mathbf{r}, \mathbf{r}')$ which, in general, is non-local but can be approximated by an effective c.m. potential $W(r)$. The effective c.m. potential consists of two contributions, the intrinsic part $W^{\rm intr}(r) = E_\alpha^{(0)} + W^{\rm Pauli}(r)$ and the external part $W^{\rm ext}(r)$ which is determined by the mean-field interactions.

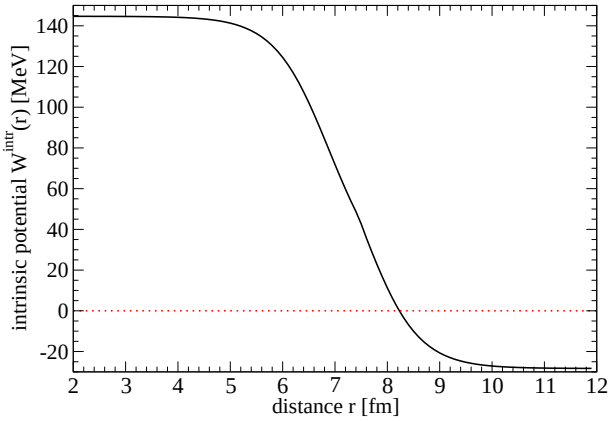

FIG. 1. Intrinsic part $W^{\rm intr}(\mathbf{r})$ of the effective c.m. potential $W(\mathbf{r})$. The empirical density distribution [9] for the ^{208}Pb core has been used. The four-nucleon Fermi energy for $r < r_{\rm cluster}$ is taken in Thomas–Fermi approximation

The intrinsic part $W^{\rm intr}(r)$ approaches for large r the bound state energy $E_\alpha^{(0)} = -B_\alpha = -28.3$ MeV of the α particle. In addition, it contains the Pauli blocking effects $W^{\rm Pauli}(r)$ given above [8]. Since the distance from the center of the lead core is now denoted by r, we have for $r > r_{\rm cluster}$ the shift of the binding energy of the α-like cluster. Here, the Pauli blocking part has the form $W^{\rm Pauli}[n_B(r)]$ given above. For $r < r_{\rm cluster}$, the density of the core nucleus is larger than the Mott density so that no bound state is formed. As lowest energy state, the four nucleons of the quartetting state are added at the edge of the continuum states that is given by the chemical potential. In the case of the Thomas-Fermi model, not accounting for an external potential, the chemical potential coincides with the sum of the four constituting Fermi energies. For illustration, the intrinsic part $W^{\rm intr}(\mathbf{r})$ in Thomas-Fermi approximation, based on the empirical density distribution, is shown in Fig. 1. The repulsive contribution of the Pauli exclusion principle is clearly seen.

The external part $W^{\rm ext}(\mathbf{r})$ is given by the mean field of the surrounding matter acting on the four-nucleon system. It includes the strong nucleon-nucleon interaction as well as the Coulomb interaction. According to Eq. (51) in [8] it is given by a double-folding potential using the intrinsic α-like cluster wave function. For $r > r_{\rm cluster}$ the simple Woods-Saxon potential used in [8] is improved in the present work using the M3Y double-folding potential [15]. This M3Y potential contains in addition to the Coulomb interaction the direct nucleon-nucleon interaction $V_N(r)$ and the

exchange terms $V_{\rm ex}(r) + V_{\rm Pauli}(r)$ [15].

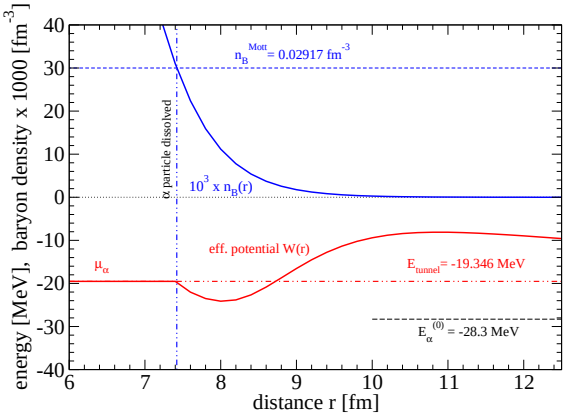

FIG. 2. Effective c.m. potential $W(r)$, potential A. The empirical baryon density distribution [9] for the ^{208}Pb core is also shown. The chemical potential μ_α coincides with the binding energy $E_{\rm tunnel}$.

The Coulomb interaction is calculated as a double-folding potential using the proton density $n_p(r)$ of the ^{208}Pb core given above and a Gaussian density distribution for the α cluster, with the charge r.m.s. radius 1.67 fm. The direct nucleon-nucleon interaction is obtained by folding the measured nucleon density distribution of the ^{208}Pb core $n_B(r)$ and the Gaussian density distribution for the α cluster (point r.m.s. radius 1.44 fm) with a parameterized nucleon-nucleon effective interaction $v(s) = c\exp(-4s)/(4s) - d\exp(-2.5s)/(2.5s)$ describing a short-range repulsion (c) and a long-range attraction (d), s denotes the nucleon-nucleon distance.

We will not perform a self-consistent calculation of the core nucleus here, but consider the potential $W(r)$ in some approximations. For comparison, three sets of c.o.m. potentials from the double-folding procedure are discussed here: Potential A, potential B, and potential C. For $r > r_{\rm cluster}$, the corresponding parameter values for c, d of the direct term $V_N(r)$ are given in Tab. I. For the exchange terms we use in case A and B the Pauli blocking $W^{\rm Pauli}[n_B(r)]$ obtained from the microscopic approach, in case C the M3Y parametrization for the exchange terms are given below. Potential A is considered to explain the physics behind our approach.

In principle, the nucleon mean field should reproduce the empirical densities of the ^{208}Pb core. For $r < r_{\rm cluster}$ a local-density (Thomas-Fermi) approach will give a constant chemical potential μ_4 which is the sum of the mean-field potential and the Fermi energy of the four nucleons, $\mu_4 = W^{\rm ext}(\mathbf{r}) + 2E_{{\rm F},n}(n_n) + 2E_{{\rm F},p}(n_p)$ with $E_{{\rm F},\tau}(n_\tau) = (\hbar^2/2m_\tau)(3\pi^2 n_\tau)^{2/3}$. This quantity is not depending on position. Additional four nucleons must be introduced at the value μ_4. We consider this property as valid for any local-density approach, the continuum edge for adding quasiparticles to the core nucleus is given by the chemical potential, not depending on position. In a rigorous Thomas–Fermi approach for the core nucleus, this chemical potential coincides with the bound state energy $E_{\rm tunnel}$ of the four-nucleon cluster, $E_{\rm tunnel} = \mu_4$. For $r < r_{\rm cluster}$, the effective c.m. potential $W(r)$ describes the edge of the four-nucleon continuum where the nucleons can penetrate into the core nucleus. Note that we withdraw this relation for shell model calculations where all states below the Fermi energy are occupied, but the next states (we consider the states above the Fermi energy as "continuum states" with respect to the intrinsic four-nucleon motion) are separated by a gap so that $E_{\rm tunnel} > \mu_4$. We come back to this issue below in the Discussion.

Potential A is designed according to this simple local-density approach. The two parameter values $c_{\rm A}, d_{\rm A}$ are determined by the conditions $\mu_4 = E_{\rm tunnel} = -19.346$ MeV, see Fig. 2. The tunneling energy is identical with the energy at which the four nucleons are added to the core nucleus. The total c.m. potential is continuous at $r = r_{\rm cluster}$ and is constant for $r < r_{\rm cluster}$, where the effective c.m. potential is $W(r) = \mu_4$. The corresponding values for the preformation factor and the decay half-life are given in Tab. I.

In a better approximation, the simple local-density (Thomas-Fermi) approach for the ^{208}Pb core nucleus has to be replaced by a shell model calculation. Then, the single-particle states are occupied up to the Fermi energy, and additional nucleons are introduced on higher energy levels according to the discrete structure of the single energy level spectrum. The condition $E_{\rm tunnel} = \mu_4$ is withdrawn. If the shell model is appropriate for the core nucleus, with the Fermi energy at μ_4, additional nucleons have a somewhat higher energy, $E_{\rm tunnel} > \mu_4$. (Note that in the opposite case a shell-model approach becomes unstable against the formation of clusters.)

Potential B is designed without the condition $\mu_4 = E_{\rm tunnel}$. The two parameter values $c_{\rm B}, d_{\rm B}$ are determined by the two empirical values bound state energy $E_{\rm tunnel} = -19.346$ MeV and the half-life$T_{1/2} = 2.99 \times 10^{-7}$ s for ^{212}Po. The

corresponding values are given in Tab. I. As expected, the bound state energy is above the value $W(r) = \mu_4$ for the c.m. potential at $r < r_{\rm cluster}$. A plot of the c.m. potential as well as the different contributions is shown in Fig. 3.

The standard version of the M3Y parametrization [15] fixes the parameter values $c_{\rm C}, d_{\rm C}$ as given in Tab. I. Instead of the Pauli blocking $\tilde{W}^{\rm Pauli}(n_B)$ used for potentials A and B, the potential C contains the M3Y exchange part $V_{\rm ex} = -276(1 - 0.005\ Q_\alpha/A_\alpha)\delta(s)$ which also accounts for the Pauli exclusion principle, as well as an additional repulsive interaction simulating the Pauli blocking [10]. The additional repulsive interaction $v^{\rm Pauli}(s) = v_{\rm rep}(s) = 470\delta(s)$ MeV is folding with a relatively density profile characterized by diffuseness parameter $a_{\rm rep} = 0.268$ fm fitted to the nuclear incompressibility $K = 220$ MeV [10]. Bound state energy, preformation factor, and half-life are calculated as shown in Tab. I.

As clearly seen in Fig. 3, all potentials A, B, and C are dominated by the Coulomb repulsion for finite distances $r \geq 15$ fm, and at large distances only the bound state energy of the free α particle remains, $\lim_{r\to\infty} W(r) = -28.3$ MeV. Below $r \approx 15$ fm, both the attractive nuclear potential and repulsive Pauli blocking between the α-particle and the lead core become relevant. At a critical distance $r_{\rm cluster} = 7.4383$ fm (where $n_B = 0.02917$ fm^{-3}), the α cluster is suddenly dissolved and the four nucleons added to the core are implemented on top of the Fermi energy μ_4 [8].

Frequency (pre-exponential factor) ν and exponential factor $\mathcal{T}$. Using the two-potential approach of Gurvitz [11], the effective c.o.m. potential $W(r)$ is separated into two parts at $r_{\rm sep} = 15$ fm (the precise choice of the separating point will almost not affect the final results). By solving the corresponding c.o.m. Schrödinger equations, both the bound state wave function $\Phi(r)$ and the scattering state wave function $\chi(r)$ are calculated. We show both $\Phi(r)$ and $\chi(r)$ obtained from potential B in Fig. 4. The c.o.m. wave function $\Phi(r)$ exhibits an approximately linear increase up to the critical distance $r_{\rm cluster} = 7.4383$ fm (where $n_B = n_B^{\rm Mott}$) and then decreases. As shown in [8], the four-nucleon intrinsic wave function $\varphi^{\rm intr}(\mathbf{s}_j, r)$ is nearly identical with the free α-particle wave function in the region $r > r_{\rm cluster}$, whereas for $r < r_{\rm cluster}$ the intrinsic wave function behaves like a product of free nucleon wave functions so that the overlap with the free α-particle wave function is nearly zero. The preformation probability of the α cluster is obtained by integrating the $\Phi(r)$ from this critical point to infinity [8]:

$$P_\alpha = \int_0^\infty d^3r |\Phi(r)|^2 \Theta\left[n_B^{\rm Mott} - n_B(r)\right] \tag{1}$$

The scattering state wave function $\chi(r)$ exhibits a strong oscillating feature as a combination of regular and irregular Coulomb functions. The decay width is then calculated by using the values of $\Phi(r)$ and $\chi_k(r)$ at the separation point. We choose $r_{\rm sep} = 15$ fm [11]:

$$\Gamma = \nu \times \mathcal{T} = \frac{4\hbar^2\alpha^2}{\mu k} |\Phi(r_{\rm sep})\chi_k(r_{\rm sep})|^2, \tag{2}$$

where $\mu = A_\alpha A_d/(A_\alpha + A_d)$, $\alpha = \sqrt{2\mu(V(r_{\rm sep}) - E_{\rm tunnel})}/\hbar$, $k = \sqrt{2\mu E_{\rm tunnel}}/\hbar$, A_d is the mass number of the lead core, and the decay half-life is related to the preformation probability and decay width by $T_{1/2} = \hbar \ln 2/(P_\alpha \Gamma)$.

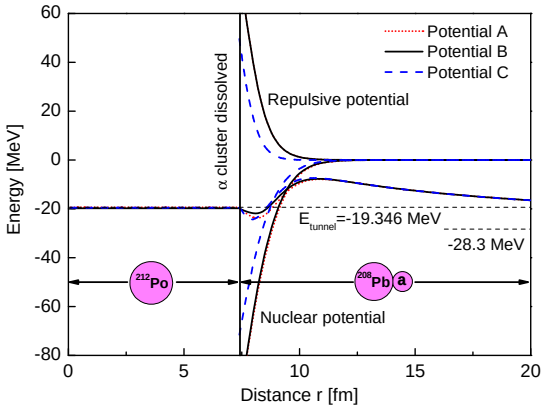

FIG. 3. Effective c.o.m. potential $W(r)$ for the α-decay of ^{212}Po. Both versions B, C give the empirical bound state energy $E_{\rm tunnel} = -19.346$ MeV, see Tab. I. The repulsive potential is given by the Pauli blocking term (Potential B) or the exchange terms (Potential C). The total c.m. potential $W(r)$ contains, in addition, the Coulomb part and the bound state energy $E_\alpha^{(0)} = -28.3$ MeV. The chemical potential μ_4 is slightly deeper than the bound state energy $E_{\rm tunnel} = -19.346$ MeV, see Tab. I.

Results. In Table I, the details of the calculated preformation probability and decay half-life of ^{212}Po are presented. All potentials A, B, and C are designed (parameter values c, d for A, B, or exchange potential for C) so that the

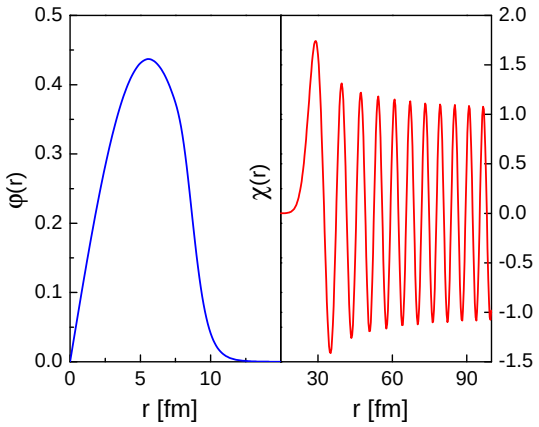

FIG. 4. The bound state wave function $\Phi(r)$ and the scattering state wave function $\chi(r)$ calculated by separating potential B into two parts based on the two-potential approach. The separating point is chosen to be $r_{\rm sep} = 15$ fm.

experimental bound state energy $E_{\rm tunnel} = Q_\alpha - 28.3 = 8.954 - 28.3 = -19.346$ MeV is reproduced. If the Thomas-Fermi condition $E_{\rm tunnel} = \mu_4$ is fixed (potential A), the calculated half-life $T_{1/2}$ is too short. The measured decay half-life $T_{1/2}$=2.99×10^{-7} s is used to design potential B. The corresponding Fermi energy of potential B is $\mu_\alpha = -19.771$ MeV and the α-cluster preformation factor is $P_\alpha = 0.142$. It is emphasized that the preformation factor and decay half-life of ^{212}Po are consistently computed in a microscopic way, but the potential B was chosen (parameter values $c_{\rm B} = 11032.08$ MeV fm and $d_{\rm B} = 3415.56$ MeV fm) to fit these empirical data. The parametrization of potential C used is taken from the literature [10], modified by fitting the experimental binding energy. The calculated half-life $T_{1/2}$ is below the experimental value. The α-cluster preformation factor, which is the most difficult part in the α-decay theory, is now well constrained by the experimental data.

By varying the strength parameter v^0 of the additional repulsive interaction in potential C $v_{\rm rep}(s) = v^0\delta(s)$ MeV while keeping other parameters fixed, it is observed that the decay half-life is mainly determined by the energy eigenvalue $E_{\rm tunnel}$ (or decay energy). This is consistent with previous α-decay calculations. To show this behavior more clearly, the correlation between the energy eigenvalue $E_{\rm tunnel}$ and the decay half-life $T_{1/2}$ is given in the left panel of Fig. 5 with various parameter values. Comparing potentials A, B, and C, it is also observed that the α cluster preformation factor depends closely on the difference between the the energy eigenvalue $E_{\rm tunnel}$ and the Fermi energy μ_4. A systematic dependence of the preformation factor on $E_{\rm tunnel} - \mu_4$ is shown in the right panel of Fig. 5.

TABLE I. The calculated preformation probability and decay half-life of ^{212}Po using different sets of effective c.o.m. potentials.

Potential	c [MeV fm]	d [MeV fm]	exchange term	$E_{\rm tunnel}$ [MeV]	Fermi energy μ_4[MeV]	$E_{\rm tunnel} - \mu_4$ [MeV]	Preform. factor P_α	Decay half-life $T_{1/2}$[s]
A	13866.30	4090.51	$W^{\rm Pauli}(n_B)$	-19.346	-19.346	0	0.367	2.91×10^{-8}
B	11032.08	3415.56	$W^{\rm Pauli}(n_B)$	-19.346	-19.771	0.425	0.142	2.99×10^{-7}
C	7999	2134	$V_{\rm ex} + V_{\rm Pauli}$	-19.346	-19.490	0.144	0.268	1.11×10^{-7}

Discussion. We neglected gradient terms so that our approach is close to the local-density approximation. We have to remember that within a rigorous approach the c.m. potential $W(\mathbf{r}, \mathbf{r}')$ is non-local. A full treatment of the inhomogeneous case relevant for finite nuclei, which includes the gradient terms and the non-local potentials, is a future goal, presently not in reach.

In addition, the relation (1) for the preformation probability is only a simple approximation. An improved approach for the intrinsic wave function $\varphi^{\rm intr}(\mathbf{s}_j; \mathbf{R})$, with a smooth behavior at $r_{\rm cluster}$ to replace the step function $\Theta\left[n_B^{\rm Mott} - n_B(r)\right]$, will modify the result for P_α.

The core is described by an uncorrelated quasiparticle model, the Thomas-Fermi model or nuclear shell model with a Fermi energy. Also pairing correlations can be introduced. It is an important question to improve the description of the core, allowing also for correlations. This would affect the questions about the potential and the wave function for $r < r_{\rm cluster}$ where a constant Fermi energy or chemical potential μ_4 was considered. Instead, the c.o.m. potential $W(r)$ and consequently the wave function $\Phi(r)$ will depend on r in a more complex way also for $r < r_{\rm cluster}$. Presently, there are different attempts (FMD, AMD, etc.) to include few-nucleon correlations to calculate light nuclei. The treatment

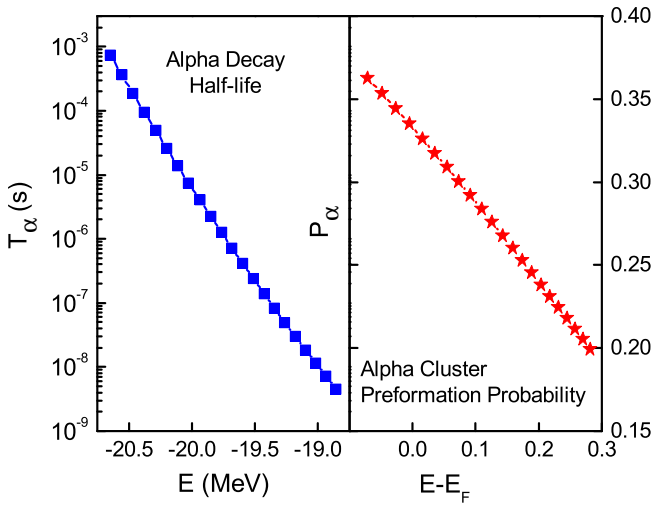

FIG. 5. The variation of the decay half-life $T_{1/2}$ with the energy eigenvalue $E_{\rm tunnel}$ (left panel) and the variation of preformation factor with the difference between the the energy eigenvalue $E_{\rm tunnel}$ and the Fermi energy μ_4 (right panel).

of heavier nuclei is not feasible with present computer capabilities.

The approach is inspired by the THSR wave function concept that has been successfully applied to light nuclei. Shell model calculations are improved by including four-particle (α-like) correlations that are of relevance when the matter density becomes low. A closer relation of the calculation presented here to the THSR calculations is of great interest, see the calculations for ^{20}Ne [16, 17]. Related calculations are performed in Ref. [18]. The comparison with THSR calculations would lead to a better understanding of the microscopic calculations, in particular the c.o.m. potential, the c.o.m. wave function, and the preformation factor.

(Note that the position of the chemical potential determines the preformation probability. If $\mu_4 < E_{\rm tunnel}$, the preformation probability becomes smaller. If $\mu_4 > E_{\rm tunnel}$, the preformation probability becomes larger. In the latter case, the states at the Fermi surface are also correlated. This is the case, e.g., for the Hoyle state where all nucleons are found in correlated states.)

[1] D. S. Delion, R. J. Liotta, and R. Wyss, Phys. Rev. C **92**, 051301(R) (2015).
[2] A. Tohsaki, H. Horiuchi, P. Schuck, and G. Röpke, Phys. Rev. Lett. 87, 192501 (2001).
[3] J. A. Wheeler, Phys. Rev. **52**, 1083 (1937).
[4] D. L. Hill, J. A. Wheeler, Phys. Rev. **89**, 1120 (1953).
[5] M. Chernykh, H. Feldmeier, T. Neff, P. vonNeumann- Cosel, and A. Richter, Phys. Rev. Lett. **98**, 032501 (2007) and refs therein.
[6] Y. Kanada-En'yo, Progr. Theor. Phys. **117**, 655 (2007) and refs therein.
[7] K. Varga, R.G. Lovas, and R. J. Liotta, Phys. Rev. Lett. **69**, 37 (1992).
[8] G. Röpke, P. Schuck, Y. Funaki, H. Horiuchi, Zhongzhou Ren, A. Tohsaki, Chang Xu, T. Yamada, and Bo Zhou, Phys. Rev. C **90**, 034304 (2014).
[9] C. M. Tarbert *et al.*, Phys. Rev. Lett. **112**, 242502 (2014).
[10] S. Misicu and H. Esbensen, Phys. Rev. C **75** , 034606 (2007); **76**, 054609 (2007).
[11] S. A. Gurvitz, Phys. Rev. A **38**, 034304 (1988); S. A. Gurvitz and G. Kalbermann, Phys. Rev. Lett. **59**, 262, (1987).
[12] Y. Ren and Z. Ren, Phys. Rev. C **85**, 044608 (2012);C. Xu and Z. Ren, Phys. Rev. C **74**, 014304 (2006).
[13] V. Yu. Denisov and A. A. Khudenko, Phys. Rev. C **79**, 054614 (2009).
[14] S. Typel, Phys. Rev. C **89**, 064321 (2014).
[15] G. R. Satchler and W. G. Love, Phys. Rep. **55**, 183 (1979).
[16] Bo Zhou, Zhongzhou Ren, Chang Xu, Y. Funaki, T. Yamada, A. Tohsaki, H. Horiuchi, P. Schuck, and G. Röpke, Phys. Rev. C **86**, 014301 (2012).
[17] Bo Zhou, Y. Funaki, H. Horiuchi, Zhongzhou Ren, G. Röpke, P. Schuck, A. Tohsaki, Chang Xu, and T. Yamada, Phys. Rev. C **89**, 034319 (2014).
[18] W. Horiuchi and Y. Suzuki, Phys. Rev. C **89**, 011304(R) (2014).